Non-sequential double ionization of helium and related wave-function dynamics obtained from a five-dimensional grid calculation.

H.G. Muller

FOM-Institute for Atomic and Molecular Physics
Kruislaan 407, 1098 SJ Amsterdam, The Netherlands

muller@amolf.nl
http://www.amolf.nl/

Abstract: Numerical integration of the time-dependent Schrödinger equation for two three-dimensional electrons reveals the behavior of helium in the presence of strong 390 nm and 800 nm light. Non-sequential double ionization is seen to take place predominantly at times when the electric-field component of the light reaches its peak value. Double ionization starts only in the second cycle of a flat-top pulse, and reaches a stable value only after many cycles, showing that recollision, sometimes through very long trajectories, must be involved.

OCIS codes: (020.0020) Atomic and molecular physics; (270.6620) Strong-field processes

References and links

1. N.B. Delone and V.P. Krainov, "Tunneling and barrier suppression ionization of atoms and ions in a laser radiation field," Phys.-Uspekhi **41**, 469 (1998).
2. S. Augst, D. Strikland, D. Meyerhofer, S.L. Chin, J. Eberly, "Tunneling ionization of noble gases in a high-intensity laser field," Phys. Rev. Lett. **63**, 2212 (1989).
3. P. Lambropoulos, "Mechanisms for multiple ionization of atoms by strong laser pulses," Phys. Rev. Lett. **55**, 2141 (1985).
4. B. Walker, B. Sheehy, L.F. DiMauro, P. Agostini, K.J. Schafer and K.C. Kulander, "Precision measurement of strong field double ionization," Phys. Rev. Lett. **73**, 1227 (1994);
5. A. l'Huillier, A. Lompre, G. Mainfray, and C. Manus, "Multiply charged ions induced by multiphoton absorption in rare gases at 0.53 μm," Phys. Rev. A **27**, 2503 (1983).
6. P. Corkum, "Plasma perspective on strong field multiphoton ionization," Phys. Rev. Lett. **71**, 1994 (1993).
7. D.N. Fittinghoff, P.R. Bolton, B. Chang, and K.C. Kulander, "Observation of nonsequential double ionization of helium with optical tunneling," Phys. Rev. Lett. **69**, 2642 (1992).
8. J.S. Parker, L.R. Moore, D. Dundas and K.T. Taylor, "Double ionization of helium at 390 nm," J. Phys. B **33**, L691 (2000).
9. E.S. Smyth, J.S. Parker, K.T. Taylor, "Numerical integration of the time-dependent Schrödinger equation for laser-driven helium," Computer Phys. Comm. **114**, 1 (1998).
10. K.J. Schafer and K.C. Kulander, "Energy analysis of time-dependent wave functions: Application to above-threshold ionization," Phys. Rev. A **42**, 5794 (1992).
11. H.G. Muller, "Solving the time-dependent Schrödinger equation in five dimensions,' in L.F. DiMauro, R.R. Freeman, and K.C. Kulander (eds.) "*Multiphoton processes: ICOMP VIII, 8th International Conference*," CP525, p. 257 AIP, Melville NY (2000).
12. H.G. Muller, "An efficient propagation scheme for the time-dependent Schrödinger equation in the velocity gauge," Laser Phys. **9**, 138 (1999).
13. H.G. Muller, "Numerical solution of high-order ATI enhancement in argon," Phys. Rev. A **60**, 1341 (1999).
14. H.G. Muller, "Calculation of double ionization of helium," in B. Piraux et al. (eds.) "Super-Intense Laser-Atom Physics VI proceedings," NATO series B (2001) in print.
15. J.L. Krause, K.J. Schafer and K.C. Kulander, "Calculation of photoemission from atoms subject to intense laser fields," Phys. Rev. A **45**, 4998 (1992).

#30932 - $15.00 US
Received February 05, 2001; Revised February 23, 2001

16. R. Kopold, W. Becker, and D.B. Milosevic, "Quantum orbits: a space-time picture of intense-laser-induced processes in atoms," Comments At. Mol. Phys. (2000) to be published.
17. H.G. Muller and F.C. Kooiman, "Bunching and Focusing of Tunneling Wave Packets in Enhancement of High-Order ATI," Phys. Rev. Lett. **81**, 1207 (1998).
18. H.G. Muller, "Identification of states responsible for ATI enhancement in argon by their calculated wave functions," Opt. Express **8**, 44 (2001).
19. J.B. Watson, A. Sanpera, K. Burnett, D.G. Lappas and P.L. Knight "Double ionization of helium beyond the single electron active electron approximation," in P. Lambropoulos and H. Walther, (eds.) "*Multiphoton Processes: ICOMP VII, 7th International Conference*," CS154, p. 132 IOP, Bristol, UK (1997).

If a multi-electron atom is subjected to intense electro-magnetic radiation, it can lose some of its electrons by ionization. Since the ionization potential IP increases even for 'equivalent' electrons roughly proportional to final-state ionic charge Z, successive electrons are more tightly bound, and therefore difficult to remove. Optical frequencies are already quite small compared to the ionization potential of neutral noble-gas atoms, and this is even more true for the higher charge states. As a consequence, the instantaneous ionization rates do not differ too much from those for ionization by a DC field[1], and this latter rate only becomes large at intensities where the electric field is strong enough to pull the electron out of the atom against the nuclear attraction[1]. This makes the intensities required to drive successive ionization steps so different, that the earlier step proceeds to completion before the next one becomes measurable[3], even for the shortest laser pulses that can be realized by current technology.

The discovery of a detectable amount (about 1 part in 10^3) of double ionization of helium at intensities below the saturation of the single ionization thus was quite surprising[4]. The production of these He^{2+} ions seems closely correlated with the presence of neutrals, suggesting that their mechanism of formation involves the simultaneous removal of two electrons. The occurrence of such 'direct' or 'nonsequential' double ionization is now known to be quite common for the noble gases, and indeed speculations about the rate of the direct process exceeding that of the second step of the sequential one are as old as 1983[5].

The precise production mechanism of the non-sequential process has not yet been elucidated. Two mechanisms were proposed, but neither of them seems to explain the experimental data satisfactorily. In the recollision model[6], the photo-electron of the first ionization step is driven back by the laser onto its parent ion at high velocity, to cause double ionization through an $(e, 2e)$ event. Alternatively, the 'shake-off' mechanism[7] assumes that the first electron leaves so rapidly that the remaining electron can not adapt its wave function adiabatically to the new situation, and gets partly excited to higher states (which either are themselves continuum, or ionize almost instantaneously).

The shake-off model does not explain why non-sequential double ionization should have the observed strong polarization dependence, which follows quite naturally from recollision: even a slight ellipticity of the polarization causes the returning electron to miss the ion. On the other hand, double ionization seems to be present even when the returning electron does not have enough energy to cause the $(e, 2e)$ process. Classical trajectory calculations show that this return energy is limited[6] to $3.17U_P$ [2]. For instance, in the case of 390-nm light at an intensity $6.5 \cdot 10^{14}\mathrm{W/cm^2}$, the ponderomotive energy U_P is only 0.36 Hartree, and the maximum return energy is barely half of what is needed to dislodge the remaining 1s electron of He^+ (which is bound by 2 Hartree).

[1]Ignoring level shifts this happens at $I = U_o^4/16Z^2$, where Z is the final ion charge; [2]. (We use atomic units $m_e = \hbar = e = 1$ unless stated differently.)

[2]Here $U_P = E_0^2/4\omega^2$ denotes the cycle-averaged kinetic energy a free electron would get due to the quiver motion forced upon it by the laser.

#30932 - $15.00 US Received February 05, 2001; Revised February 23, 2001

Nevertheless, the non-sequential yield is $3 \cdot 10^{-4}$ of that of the single ionization, or 30% of the value the double/single ratio has at saturation of the single ionization[8].

Computer technology has now progressed to a point where generating solutions with arbitrary precision for a two-electron system in three dimensions becomes a feasible proposition[9]. In this paper we study the ionization of helium by numerically integrating the time-dependent Schrödinger equation[10] for two (three-dimensional) electrons,

$$i\partial t\Psi = (\frac{1}{2}p_1^2 + \frac{1}{2}p_2^2 + V(\mathbf{r}_1, \mathbf{r}_2) + \mathbf{A}(t) \cdot \mathbf{p}_1 + \mathbf{E}(t) \cdot \mathbf{r}_2)\Psi. \quad (1)$$

For helium the atomic potential in this equation is given by $V = -2/r_1 - 2/r_2 + 1/r_{12}$. For reasons of efficiency, the two electrons are treated in different electromagnetic gauges[11]; the solution for Ψ obtained that way is related to that of the more common pure gauges by a simple multiplicative factor $\exp(i\mathbf{A}(t)\cdot\mathbf{p}_i)$ for one of the electrons. Cylindrical symmetry (around the direction of the collinear vectors $\mathbf{A}$ and $\mathbf{E}$) reduces the problem to a five-dimensional one, which is treated in spherical coordinates. The two radial dimensions r_1 and r_2 are represented on a grid of constant spacing δr, with an implicit three-point finite-difference approximation for the corresponding momentum operators[12]. The dependence on the three angular dimensions ϑ_1, ϑ_2 and ϕ_{12} is expressed on a basis $\Upsilon_{l_1 l_2 m}$ of appropriately symmetrized products of spherical harmonics,

$$\Upsilon_{l_1 l_2 m} = (Y_{l_1}^m(\vartheta_1, \phi_{12})Y_{l_2}^{-m}(\vartheta_2, \phi_{12}) + Y_{l_1}^{-m}(\vartheta_1, \phi_{12})Y_{l_2}^m(\vartheta_2, \phi_{12}))/\sqrt{2}. \quad (2)$$

Equation 1 is solved on a 'strip' $0 < r_1 < R_{out}$; $0 < r_2 < R_{in}$, where in $r_1 = 0$ and $r_2 = 0$ the boundary condition prescribed by the Coulomb singularity in V is enforced. At the other boundaries (nearly) reflectionless absorption of the wave function takes place by specially tailored boundary conditions[14], that keep track of the amount of probability they absorb. In the present calculation, R_{in} is chosen very small (8 Bohr), and current absorbed at the $r_2 = R_{in}$ boundary for $r_1 > R_{in}$ is counted as double ionization. The strip is much larger in the r_1 dimension ($R_{out} \approx 36$ Bohr, plus an absorbing region of 11 Bohr), allowing electron 1 to perform its full dynamics of laser acceleration and recollision. Only when r_1 gets so large that there is no hope of future collisions it meets the absorber. Current leaving the strip at $r_1 = R_{out}$ is counted as single ionization without examining its dependence on r_2, since any population that did not have electron 2 in the ground state would be pulled by the laser over the $r_2 = R_{in}$ boundary long before r_1 could reach R_{out}. Exchange symmetry (corrected for the gauge difference between the electrons) can be enforced on the boundary $r_1 = r_2$[11].

Because of the limited extension of the strip in the r_2 direction, together with the use of the length gauge in this dimension, only few angular momenta are required to represent electron 2. In the current calculations, l_2 running upto 4 was enough to converge all quantities except angular distributions to better than a percent. (The latter require 2 more l_2.) This also limits the theoretically required number of m to 4 , but in practice including $m \geq 2$ did not affect any of the presented results visibly where tried[3]. Due to the high spatial order of the finite-differences employed, good convergence is already obtained for $\delta r = 0.25$ Bohr, provided that the ionization potentials are tuned to their limit values by tweeking the boundary condition[15, 9] at $r_i = 0$ and at $r_1 = r_2$. The number of l_1 required varies strongly with laser parameters, and a typical value is 20. This brings the grid requirements to $188 \times 32 \times 20 \times 5 \times 2$, or about 1.2 million points.

Propagation on this grid is implemented as a multiple split-operator scheme, each partial propagator being implemented by its half-implicit approximation $(1 - iH\tau)/(1+$

[3]Note that a grid with only two m values is topologically equivalent to that needed to describe an atom of two 2-dimensional electrons (m taking the role of parity with respect to the polarization axis).

#30932 - $15.00 US
Received February 05, 2001; Revised February 23, 2001

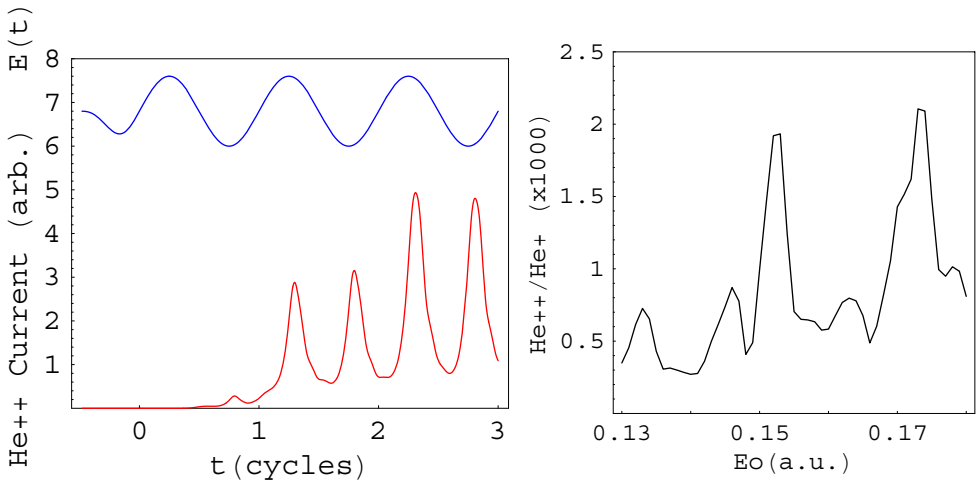

Fig. 1 The red curve gives the double-ionization rate (defined as the outward current of the innermost electron through a sphere with radius 8 Bohr). The electric field is given by the blue line, which has a constant amplitude 0.152 for $t > 0$. Similar curves for field amplitudes from 0.135 to 0.179 a.u. are stacked behind the figure as a movie (285 Kb), for easy comparison. The first burst of double ionization (at $t = 1.25$) grows monotonously with intensity. The magnitude of later bursts varies wildly due to interference with earlier ones. The right plot shows the ratio between double and single ionzation yields over cycle 5 to 10.

$iH\tau$). Thus all partial propagators are exactly unitary, and their (local) discretization error is $O(\tau^3)$. Just like in the predecessor single electron code on which this work builds[12, 13], the resulting global τ^2 convergence is maintained despite the splitting by first applying them in a certain order for half the step size, and then in the reverse order to complete a full step. The total hamiltonian is split into atomic contributions for each of the electrons (employing potentials -2/r_2 and -$(1 + (1 - r_1/2)^4_{[r_1<2]})/r_1$ for the inner and outer electron, respectively), the laser-interactions $\mathbf{E}(t) \cdot \mathbf{r}$ and $\mathbf{A}(t) \cdot \mathbf{p}$, and the first N components from the multipole expansion of the electron repulsion $1/r_{12}$. For efficiency the latter is usually only included up to the dipole moment ($N = 2$), although convergence tests have shown that results sometimes change up to 10% after inclusion of the higher multipoles. As a compromise, sometimes the higher multipoles are included only in the $m = 0$ subspace (which carries almost all population). The atomic propagators naturally factorize into tri-diagonal operators, and the other operators are split further until they do[12]. This makes propagation quite efficient, around 3.6 seconds per time step (1 optical cycle per hour) for the mentioned grid size on a 333 MHz PC.

In the first set of calculations, the atom was exposed to a flat-top laser pulse $\mathbf{E}(t) = E_0 \hat{z} \sin \omega t$, $(t > 0)$, immediately preceeded by a half-cycle sine-square turn-on[4]. The frequency ω was chosen as 0.11683, corresponding to a laser wavelength of 390 nm. This wavelength is interesting because it results in a fair amount of double ionization while the maximum return energy is still below the impact energy required for an $(e, 2e)$ process.

Fig. 1a shows the double-ionization outward current crossing the R_{in} boundary as a function of time, for various intensities around 800 TW/cm^2. This current peaks quite

[4]Even half an optical cycle is slow for the atomic ground state, so that it adapts adiabatically if the switching is smooth.

#30932 - $15.00 US
Received February 05, 2001; Revised February 23, 2001

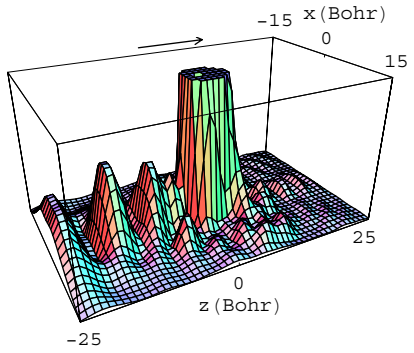

Fig. 2. One-cycle movie (1.2 Mb) of the charge distribution of the outer electron at $E_0 = 0.1525$ a.u., where the double ionization has a resonant peak.

strongly slightly after the time where the $E(t)$ reaches its maximum value. This is in agreement with earlier calculations for this process[8]. Taking account of the time needed to travel to R_{in} this suggest the corresponding electrons leave the atom at these field maxima. An interesting observation, made possible by the very steep turn-on of the pulse, is that the first burst of double ionization does appear only one full cycle after the first time a field maximum was reached. The absence of double ionization during the first cycle shows that shake-off only plays a minor role under these conditions, and points to a recollision mechanism.

Note, however, that the recollision model as originally proposed[6] would have predicted the double ionization to start a quarter cycle earlier, near an E-field zero crossing. Around that time the recollision energy is maximal (but still not high enough under these circumstances to kick out the second electron). The trajectories leading to recollision are thus longer than originally thought. At the higher intensities, a tiny secondary bump seems to develop near the zero crossings.

At some of the intensities shown, it can take as much as 10 cycles before successive ionization bursts become equal, showing that indeed very long trajectories must have significant involvement in the creation of those later bursts. Involvement of many trajectories from different durations unavoidedly causes sharp structure as a function of intensity[16, 17]. The double ionization rate is much more strongly affected by such resonance enhancement than the single one: the ratio of the two yields from the last 5 cycles in Fig. 1a is plotted in Fig. 1b and shows clear resonance peaks.

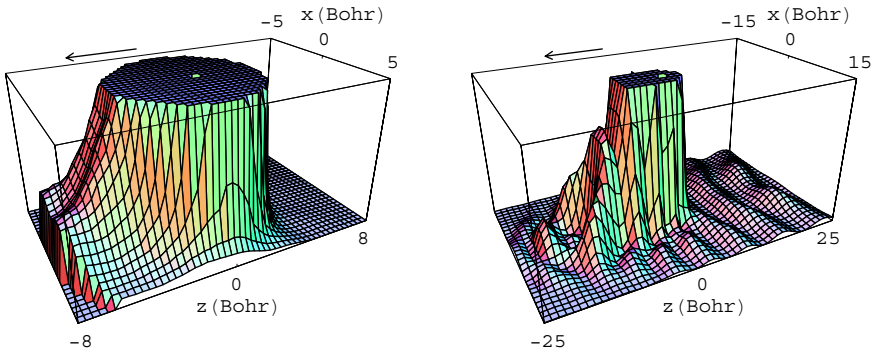

Fig. 3. The spatial distribution of the inner (left, 1.2 Mb) and outer (right, 1.3 Mb) electron in the first two cycles of the flat part of a flat-top pulse. The arrow represents the electric field vector. The circular cliff in the left movie is at the absorbing grid boundary.

#30932 - $15.00 US
Received February 05, 2001; Revised February 23, 2001

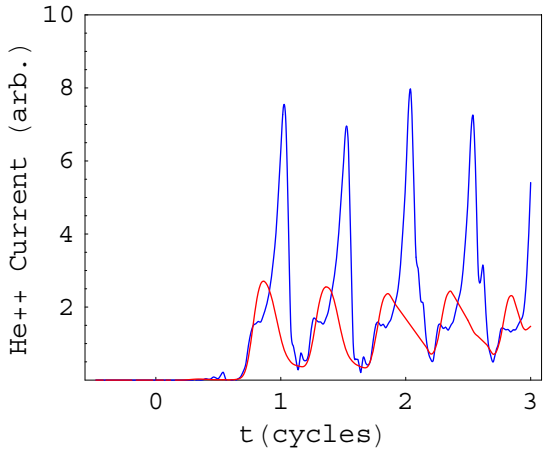

Fig. 4. Comparison of double ionization at 390 nm and 1100 TW/cm^2, for the real case (blue) and in an artificial situation where the innermost electron does not feel the laser (red). (The first full E-field peak occurs at $t = 0$.)

The charge distribution of the outer electron (integrated over all coordinates of the inner one) at the resonance intensity is shown in Fig. 2; it consists mainly of charge blobs on the polarization axis, that all recollide with the parent ion.

Fig. 3a shows a movie of the spatial distribution of the inner electron at a higher intensity (i.e. it plots the probability that one of the electrons is at the indicated location, and the other is somewhere at a larger distance from the nucleus)[5]. This inner electron leaves the atom mainly in the direction where the laser field pushes it at the time. The corresponding charge distribution of the outer electron is shown in Fig. 3b. For this calculation exchange symmetry was not enforced (for Fig. 1 it was). This treats the electrons on unequal footing; electron 1 is allowed to venture far from the atom to return later, while electron 2 is immediately and irrevokably absorbed when it leaves the close vicinity of the atom. Processes triggered only by the return of an electron will thus be underestimated (by a factor two).

Due to this breaking of electron equivalence, it becomes possible to do a very instructive test, namely to switch off the interaction between the field and electron 2[19]. In Fig. 4 it can be seen that this dramatically decreases the amount of double ionization, indicating that the field actively participates in the ionization of the second electron. The small amount of double ionization left appears well before the electric field maxima, and must be caused by energy transfer from electron 1 to electron 2. Indeed, the time at which the bursts appear are close to those times for which the initial photo-electron returns with maximum energy. In this case of slightly higher intensity (1100 TW/cm^2) this return energy is enough to kick out the inner electron if the first electron gives up more energy than it has, to end up in a He^+ bound excited state (from which it is ionized immediately afterwards). Fig. 5 plots the charge-distribution of the non-driven electron when it is the inner one. This shows that this electron still prefers to leave in the direction of the field it can not feel.

[5]For best representation of both on-axis and off-axis probability, this and later movies plot $|\Psi|^2\sqrt{\rho^2+10}$, (ρ being the distance to the axis of cylinder symmetry)[18]. All movies present the evolution during a flat part of a pulse that starts with an E-field maximum, following a half-cycle turnon. Synchronous side by side viewing of movies is encouraged.

#30932 - $15.00 US
Received February 05, 2001; Revised February 23, 2001

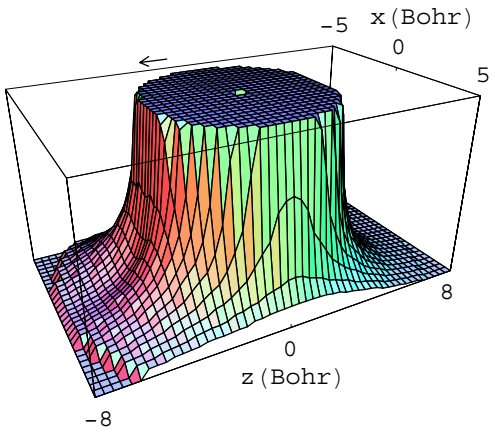

Fig. 5. A movie (1.2 Mb) of the innermost electron charge (similar to fig. 2a) when this electron is artificially uncoupled from the laser.

If the interaction of electron 2 with the laser is included, the ionization bursts at E-field zero crossings seem still recognizable, but only as tiny shoulders to much larger burst. Most of the double ionization current apparently emerges due to combined action of the electron repulsion and the laser field, where it is more important that the laser field is strong than that the return energy is high.

At a wavelength of 800 nm the return energy can get much higher than at 390 nm, and will easily exceed the threshold value for the $(e, 2e)$ process. The calculation is also much more demanding: because of the larger quiver amplitude R_{out} has to be chosen much larger (116 Bohr), and 30 to 50 l_1-components are required. Fig. 6 shows the double ionization at 505 TW/cm^2, where $U_P = 1.1$ Hartree (which makes maximum return energy 3.5 Hartree). The double ionization is now much less localized to the E-field maxima, and switches on at the zero crossing 0.75 cycle after the first maximum. Nevertheless, there is still a distinct peak at the E-field maxima, that starts to dominate

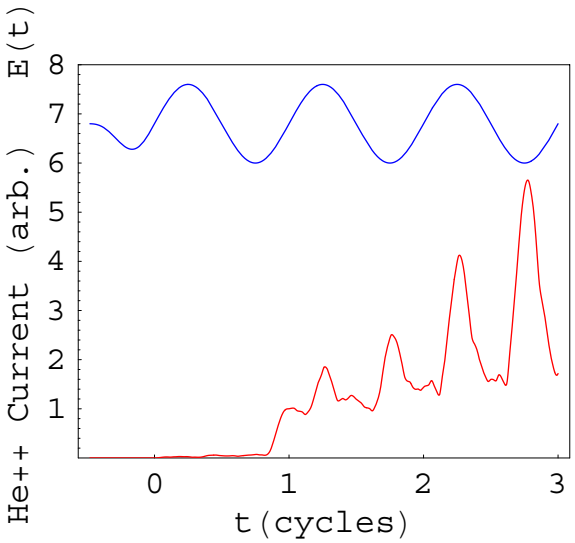

Fig. 6. Double ionization current at 800 nm, 505 TW/cm^2, and E field causing it.

#30932 - $15.00 US
Received February 05, 2001; Revised February 23, 2001

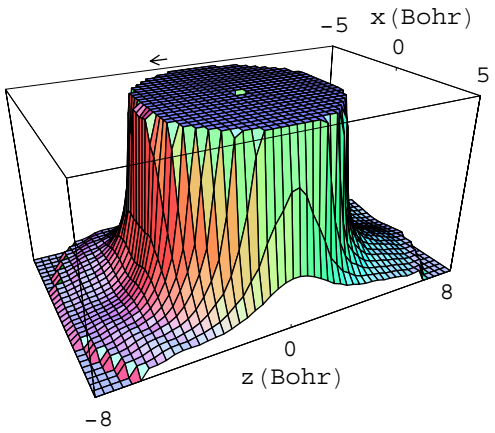

Fig. 7. A movie (1.2 Mb) of the innermost electron charge distributions at 800 nm, 1000 TW/cm^2. The electron repulsion was only included upto the dipole term.

in later cycles. Apparently very long trajectories also play an important role here, but due to the expensive nature of the calculation no systematic intensity scan for locating resonances could yet be undertaken (a 5-cycle run now takes over 2 days).

Finally the movie of Fig. 7 shows the charge distribution of the inner electron at 800 nm and 1000 TW/cm^2. At this intensity l_1 has to run upto 50 and 4000 steps per optical cycle are required to obtain convergence. The double-ionization current also shows a strongly directional component at this intensity, that peaks around the field maxima. Unlike in the other movies shown, this contribution originates mainly from situations where the outer electron is very far away. It seems quite independent of where the outer electron exactly is: from $r_1 = 50$ to $r_1 = R_{out} = 127$ Bohr the current of the second electron leaving the ion at the time of an E-field maximum is practically constant. In other words, the contribution near these field maxima seems to correspond to sequential double ionization.

There is also a non-sequential component to the double ionization, and it is located strongly around the E-field zero crossings, and it only emerges when the first electron is close by ($r_1 < 50$ Bohr). In Fig. 7 this current can be seen to be much more isotropic, leaving in all directions at the same time. (Note that this does not reveal anything about the final momentum of the electrons, which is mainly determined by the phase of the laser at the time of emission.)

Acknowledgement - This work is part of the research program of FOM (Fundamental Research on Matter), which is subsidized by NWO (Netherlands Organization for the advancement of Research). I want to express my gratitude to the people of Ken Taylor's group at the Queen's University, and in particular to Laura Moore, for answering my load of questions about details of their work. Matt Kalinski helped me in preparing the movies.